

# Geometry of frictionless and frictional sphere packings

Leonardo E. Silbert<sup>1</sup>, Deniz Ertas<sup>2</sup>, Gary S. Grest<sup>1</sup>, Thomas C. Halsey<sup>2</sup>, and Dov Levine<sup>3</sup>

<sup>1</sup> Sandia National Laboratories, Albuquerque, New Mexico 87185

<sup>2</sup> Corporate Strategic Research, ExxonMobil Research and Engineering, Annandale, New Jersey 08801

<sup>3</sup> Department of Physics, Technion, Haifa, 32000 Israel

(October 29, 2018)

We study static packings of frictionless and frictional spheres in three dimensions, obtained via molecular dynamics simulations, in which we vary particle hardness, friction coefficient, and coefficient of restitution. Although frictionless packings of hard-spheres are always isostatic (with six contacts) regardless of construction history and restitution coefficient, frictional packings achieve a multitude of hyperstatic packings that depend on system parameters and construction history. Instead of immediately dropping to four, the coordination number reduces smoothly from  $z = 6$  as the friction coefficient  $\mu$  between two particles is increased.

## I. INTRODUCTION

Dense amorphous packings of frictionless spheres have proven to be an extremely useful paradigm in different physical contexts, such as metallic glasses [1], colloidal crystals [2], and emulsion rheology [3]. Granular materials are another example of a system with macroscopically large particles, with one major difference: grain-grain interactions involve frictional forces. As a result, granular packings may be quite different from frictionless sphere packings in ways which may impact significantly on their physical properties.

A common quantity of interest in packings of hard spheres is the average number of contacts per particle (coordination number)  $z$ . In order to achieve static mechanical equilibrium, each sphere in the packing needs a sufficient number of constraints that freeze out its translational and rotational degrees of freedom. These constraints are provided by contacts, and once there are a sufficient number of them, the packing can accommodate external body or boundary forces, as long as a set of contact forces satisfying mechanical equilibrium can be found for the given arrangement of such contacts. The minimal average coordination number required to obtain static packings of  $d$ -dimensional frictionless spheres that are stable against external perturbations is  $z_n = 2d$  [4], whereas for spheres with friction,  $z_f = d + 1$  [5]. In three dimensions,  $z_n = 6$  and  $z_f = 4$ . We call such packings “isostatic”.

In this study, we investigate whether or not sphere packings readily achieve isostaticity under generic packing conditions. This isostaticity hypothesis is important in theories focusing on the macroscopic response of such packings [6], and at first appears reasonable, given the strong numerical evidence from simulation [3,7] that  $z_n = 6$  for dense random packings of frictionless spheres. Simulation studies of frictional spheres compressed in a gravity-free environment [7] have shown that  $z_f$  is significantly less than 6, but with the lowest achieved value of around 4.5, it remains unclear whether the minimal value of 4 is reached in the limit of zero confining pressure

(equivalent to the hard-sphere limit.) It is also unclear in what way the packings would change for arbitrarily small friction coefficient  $\mu$  between the spheres in order to achieve a reduction in  $z$  to four, if the isostaticity hypothesis were true.

To address such questions, we perform a systematic simulation study of the effect of various parameters on sphere packings. In particular, we vary the following materials properties: the sphere hardness  $k_n$ , the coefficient of restitution  $\epsilon$ , and the friction coefficient  $\mu$  between two particles. We also vary the initial conditions of the packing by varying the initial packing density  $\phi^i$ , as well as the initial velocities of the spheres. We investigate how the density, coordination number and the nature of the contacts change as these parameters are varied. Although frictionless hard-spheres appear to form isostatic packings regardless of construction history and restitution coefficient, frictional hard-spheres achieve a multitude of hyperstatic packings ( $z > z_f$ ) that depend on system parameters and construction history [8]. The coordination number reduces smoothly from  $z = 6$  as the friction coefficient is increased, disagreeing with the isostaticity hypothesis.

## II. SIMULATION METHOD

We present molecular dynamics (MD) simulations in three dimensions on model systems of  $N = 20,000$  monodisperse, cohesionless spheres of diameter  $d$  and mass  $m$ . The system is spatially periodic in the  $xy$ -plane, with a unit cell of size  $20d \times 20d$ , and is bounded in the  $z$ -direction by a rough bed at the bottom and an open top. The starting configurations consist of randomly positioned non-overlapping spheres, with packing fractions in the range  $0.02 < \phi^i < 0.3$ , obtained by varying the overall height while keeping  $N$  and the  $x, y$  dimensions fixed. The system is subsequently allowed to settle under gravity on top of the rough bed (see Fig. 1). The equilibrated static packing height is about  $50d$ . This method of construction mimics the pouring of granular

materials through a sieve to an area far away from side walls, without forming a conical heap.

Different ways of preparing static granular packings include compressing them [7], and reducing the inclination angle of gravity-driven chute flows below the angle of repose [8]. In the frictionless case, conjugate gradient methods have been used to study dense random packings [3,9]. However, for the case of particles with friction, MD simulations are more appropriate in order to properly account for both the normal and tangential forces, since the latter depend on the loading history of the contact.

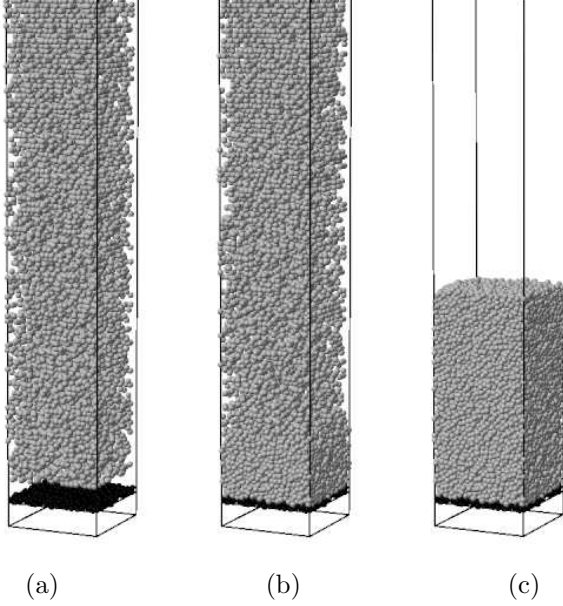


FIG. 1. Lower portion of the packing of  $N = 20,000$  spheres in a periodic cell  $20d \times 20d$  supported by a rough bed (black particles), constructed by settling under gravity, with  $\mu = 0.50$ ,  $k_n = 2 \cdot 10^5 mg/d$ , and  $\epsilon = 0.88$ . (a) Initial configuration with volume fraction  $\phi^i \approx 0.13$ . (b) Intermediate time during settling. (c) Final (static) configuration with  $\phi^f \approx 0.60$ . The black frame is added as a guide to the eye.

The spheres interact only on contact through a linear spring-dashpot interaction law [10] in the normal and tangential directions to their lines of centers [11,12]. Contacting spheres  $i$  and  $j$  positioned at  $\mathbf{r}_i$  and  $\mathbf{r}_j$  experience a relative normal compression  $\delta = |\mathbf{r}_{ij} - d|$ , where  $\mathbf{r}_{ij} = \mathbf{r}_i - \mathbf{r}_j$ , which results in a force

$$\mathbf{F}_{ij} = \mathbf{F}_n + \mathbf{F}_t. \quad (1)$$

The normal and tangential contact forces are given by

$$\mathbf{F}_n = k_n \delta \mathbf{n}_{ij} - \frac{m}{2} \gamma_n \mathbf{v}_n, \quad (2)$$

$$\mathbf{F}_t = -k_t \Delta \mathbf{s}_t - \frac{m}{2} \gamma_t \mathbf{v}_t, \quad (3)$$

where  $\mathbf{n}_{ij} = \mathbf{r}_{ij}/r_{ij}$ , with  $r_{ij} = |\mathbf{r}_{ij}|$ ,  $\mathbf{v}_n$  and  $\mathbf{v}_t$  are the normal and tangential components of the relative surface velocity, and  $k_{n,t}$  and  $\gamma_{n,t}$  are elastic and viscoelastic constants respectively.  $\Delta \mathbf{s}_t$  is the elastic tangential displacement between spheres, obtained by integrating surface relative velocities during elastic deformation of the contact. The magnitude of  $\Delta \mathbf{s}_t$  is truncated as necessary to satisfy a local Coulomb yield criterion  $F_t \leq \mu F_n$ , where  $F_t \equiv |\mathbf{F}_t|$  and  $F_n \equiv |\mathbf{F}_n|$ . Frictionless spheres can be simulated simply by setting  $\mu = 0$ . Finally, the particles are moved according to the total forces and torques applied to them through contacts and the gravitational field. Additional details can be found in Ref. [13].

The presented simulations were carried out for a range of materials parameters. The normal spring constant  $k_n$  varied from  $2 \cdot 10^5$  to  $2 \cdot 10^9 mg/d$  in order to understand how the system behaves as it approaches the hard sphere limit. In all cases,  $k_t = 2k_n/7$  [14]. In order to study the crossover from frictionless to frictional systems, the local particle friction coefficient  $\mu$  was varied from 0 to 10. Finally the coefficient of restitution  $\epsilon$ , i.e. the ratio of the final to initial normal velocities in a head-on binary collision, was also varied. For a linear spring-dashpot interaction,

$$\epsilon = \exp(-\gamma_n t_{col}/2), \quad (4)$$

where the collision time  $t_{col}$ ,

$$t_{col} = \pi(2k_n/m - \gamma_n^2/4)^{-1/2}. \quad (5)$$

Three values of  $\epsilon=0.26$ ,  $0.50$ , and  $0.88$  were used. The effect of  $\epsilon$  is like that of varying the quench rate in a thermal system: for smaller values of  $\epsilon$ , collisions are more inelastic, energy is dissipated faster, and the spheres have less ability to move from the first position where they are mechanically stable, which may result in packings that are less stable than similarly prepared packings of more elastic grains.

Most of the simulations were started from a static configuration of  $\phi^i \approx 0.13$  as shown in Fig. 1(a). The timestep  $\delta t \approx 0.05 \sqrt{m/k_n}$  was chosen to accommodate the decreasing collision time as the particle hardness  $k_n$  is increased [cf. Eq. (5)]. For  $k_n = 2 \cdot 10^5 mg/d$ ,  $\delta t \approx 10^{-4} \sqrt{d/g}$ . Simulations were then run until the kinetic energy per particle was less than  $10^{-8} mgd$  for small  $k_n$ , and up to three orders of magnitude less for large  $k_n$ . This requires  $3 - 8 \cdot 10^6 \delta t$  for small  $k_n$ , and  $4 - 8 \cdot 10^7 \delta t$  for  $k_n = 2 \cdot 10^9 mg/d$ .

Because of the large amount of time required to reach static equilibrium, each set of parameters was run for 1 to 5 configurations. In some cases, the particles were given an initial, random velocity with an average KE per particle of approximately  $20 - 100 mgd$ . The results were identical in all cases within sample to sample fluctuations.

### III. RESULTS

#### A. Coordination Number

Figure 2 shows the effect of friction coefficient  $\mu$  on  $z$  for  $k_n = 2 \cdot 10^5 mg/d$  and  $\epsilon = 0.88$  and  $0.26$ . For both values of  $\epsilon$ ,  $z = 6.144 \pm 0.002$  for frictionless packings. As we shall see in Sec. III C, the deviation from the isostatic value of 6 can be attributed to the finite stiffness of the spheres, the isostatic value is apparently obtained in the hard-sphere limit. However, there is no sudden drop from  $z = 6$  as friction is turned on; rather there is a gradual decrease in  $z$  to a parameter dependent minimal value, accompanied by a similar decrease in the final volume fraction  $\phi^f$  (see Fig. 3.)

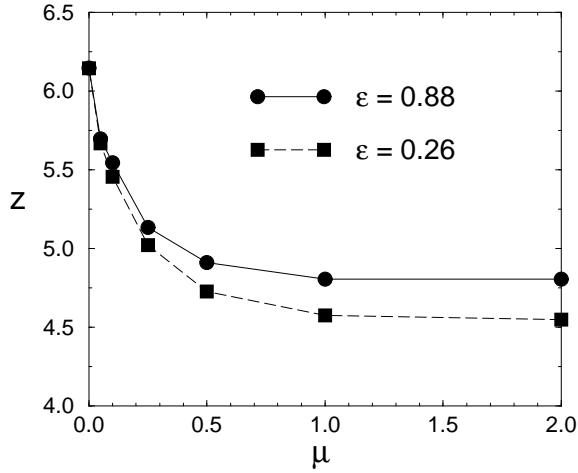


FIG. 2. Bulk averaged coordination number  $z$  as a function of  $\mu$  for  $k_n = 2 \cdot 10^5 mg/d$  and  $\phi^i = 0.13$  for two values of  $\epsilon$ .

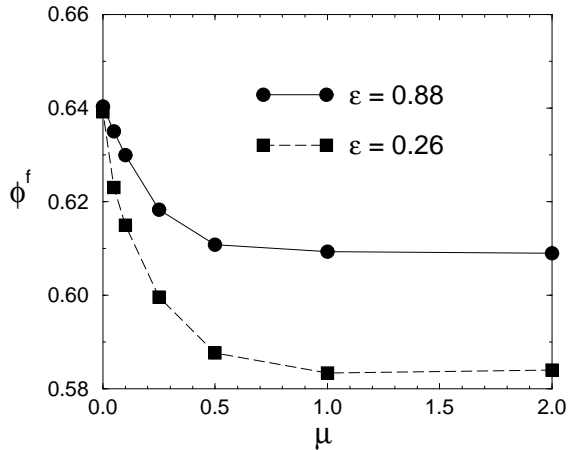


FIG. 3. Final volume fraction  $\phi^f$  versus  $\mu$  for the same parameters as in Fig. 2.

As depicted in Fig. 4, the decrease in  $z$  is primarily due to an overall shift in the distribution of coordination numbers to lower values, rather than a change in its shape and width. Consequently, the frequency of particles with eight or more neighbours reduces as  $\mu$  increases, and particles with as few as two contacts start to appear at  $\mu = 0.5$ , indicative of arching within the packing at large  $\mu$ . The saturation of  $z$  and  $\phi^f$  for  $\mu \gtrsim 1$  is due to the fact that the typical tangential forces  $F_t$  in a packing with  $\mu = \infty$  is expected to be of order  $F_n$ , and lowering  $\mu$  has little effect on the packing down to  $\mu \approx 1$ . This behavior of the contact forces is further verified in Sec. III D.

Unlike the frictionless case, the deviations from isostaticity ( $z = 4$ ) for  $\mu > 0$  cannot be attributed to corrections due to the finite stiffness of the spheres. The packings remain unambiguously hyperstatic in the hard-sphere limit.

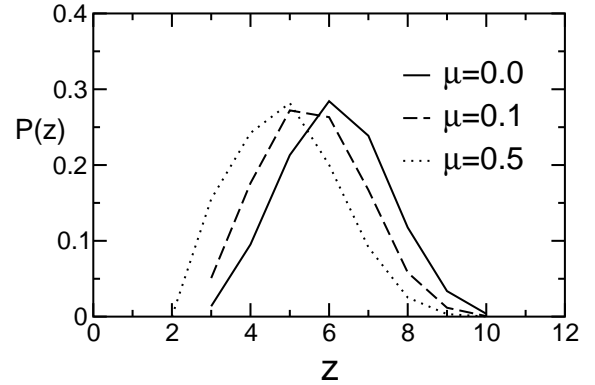


FIG. 4. Distributions of the coordination number shift to lower values of  $z$  as  $\mu$  is increased. These results are for  $k_n = 2 \cdot 10^5 mg/d$ ,  $\epsilon = 0.88$  and  $\phi^i = 0.13$ .

When a static packing with a surface tilt near the angle of repose was generated by cessation of flow down an inclined plane [8], similar results for  $z$  and  $\phi$  were obtained. For  $k_n = 2 \cdot 10^5 mg/d$ ,  $\epsilon = 0.88$ , and  $\mu = 0.50$ , such packings gave  $z = 4.69$  and  $\phi = 0.594$ , compared to  $z = 4.90$  and  $\phi = 0.61$  for packings presented in this study.

#### B. The Radial Distribution Function

The radial distribution function (RDF),  $g(r)$ , for  $k_n = 2 \cdot 10^5 mg/d$  and  $\epsilon = 0.88$ , is plotted in Fig. 5 for several values of  $\mu$ . The characteristic split second peak, indicating short-range order out to second neighbors, is evident. For  $\mu = 0$ ,  $g(r)$  is essentially identical to that obtained for random close packing (RCP), at volume fraction  $\phi^f \approx 0.64$  [15]. As  $\mu$  increases, the secondary peaks in  $g(r)$  diminish, as seen in the inset.

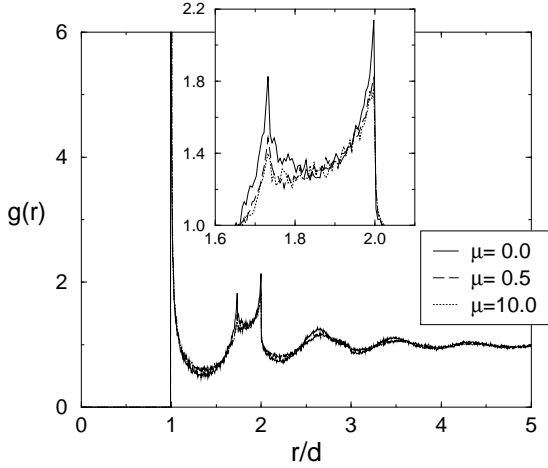


FIG. 5. The radial distribution function  $g(r)$  for spheres with and without friction for  $k_n = 2 \cdot 10^5 mg/d$  and  $\epsilon = 0.88$ .

The first peak of  $g(r)$  is of particular interest, since near-contacts with  $r/d$  just over 1 play an important role in the dependence of  $z$  on the stiffness of the spheres (See Sec. III C). Figure 6 reveals a square-root singularity of the RDF near  $r/d = 1$ , i.e.,

$$g(r) \propto \left(\frac{r}{d} - 1\right)^{-\alpha}, \quad 0 < \frac{r-d}{d} \ll 1, \quad (6)$$

with  $\alpha = 0.52 \pm 0.03$ . This singularity has apparently not been reported elsewhere, although we have also verified its presence in the RDF of hard-sphere packings provided to us [16]. Note that this singularity is integrable, and is distinct from particles actually in contact.

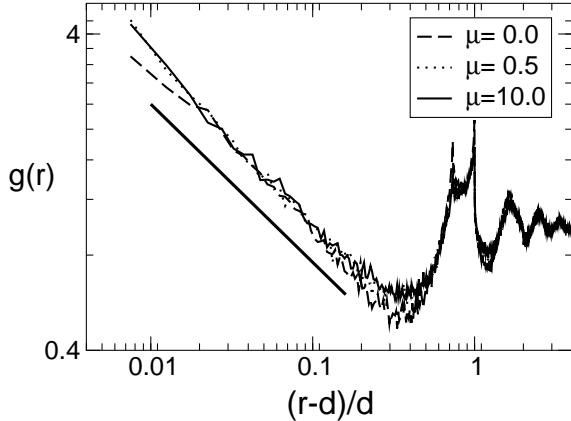


FIG. 6. A logarithmic plot of  $g(r)$  vs.  $(r-d)/d$  (for  $k_n = 2 \cdot 10^5 mg/d$  and  $\epsilon = 0.88$ ) reveals a power-law singularity with exponent  $\alpha \approx 0.5$  for both frictionless and frictional spheres. Straight line has a slope of  $-1/2$ . The same power-law is observed up to the largest values of  $k_n$  studied.

### C. The Hard-Sphere Limit

We next investigate the effect of the finite stiffness of the spheres on the packings, and on the average coordi-

ination number  $z$  in particular. Let us assume that the packings formed by these stiff elastic spheres are statistically equivalent to packings that would be obtained by first forming a truly hard-sphere packing and subsequently allowing elastic relaxation. Due to the slight compression of the spheres of finite stiffness under gravity, we expect to see an increase in coordination number during this elastic relaxation. Since the typical compressive strain of a sphere under the same loading conditions scales as  $1/k_n$ , we expect that a finite fraction of neighbors in the hard-sphere packing that were within a distance  $d[1 + O(mg/k_n d)]$  of each other form new contacts upon elastic relaxation. The number of such near-contacts in the hard-sphere packing can be computed by integrating the hard-sphere RDF  $g_\infty(r)$  over the range  $r/d \in (1, 1 + mg/k_n d)$ , yielding an effective coordination number

$$z_n(k_n) = z_\infty + \tilde{a}_n \left(\frac{k_n d}{mg}\right)^{-\alpha_n}, \quad \frac{k_n d}{mg} \gg 1, \quad (7)$$

where  $z_\infty$  is the coordination number in the hard-sphere limit,  $\tilde{a}_n$  is a constant, and the exponent [cf. Eq.(6)]

$$\alpha_n = 1 - \alpha. \quad (8)$$

Thus, there is a power-law correction to the apparent coordination number, with an exponent that depends on the nature of the singularity in the first peak of  $g(r)$ . A numerical fit of the data to Eq. (7) shown in Fig. 7(a) results in  $\alpha_n = 0.498 \pm 0.002$  and  $z_\infty = 6.01 \pm 0.02$ , in excellent agreement with the isostaticity hypothesis, as well as the exponent relation Eq. (8). Makse *et al.* also found that  $z$  approaches 6 as the stress goes to zero in their numerical studies of compressed spheres [7].

Armed with this insight, we apply a similar analysis to frictional packings, with results presented in Fig. 7(b). Although the RDF of frictional packings appears to have the same square-root divergence near  $r = d$  (see Fig. 6), the numerical fit to Eq. (7) in the presence of friction yields a different exponent  $\alpha_f \approx -1/4$ , resulting in a slower approach to the hard-sphere limit. Thus, the exponent identity Eq. (8) does not hold for frictional spheres. Moreover, in contrast to the frictionless case, the hard-sphere limits remain firmly above the isostatic value of four, and vary as a function of  $\mu$  and  $\epsilon$ .

Even though the rather unlikely scenario of a further crossover to isostaticity at extreme stiffnesses cannot be entirely ruled out, it must be pointed out that the stiffest spheres with  $k_n = 2 \cdot 10^9 mg/d$  in these packings experience strains  $\delta/d \lesssim 10^{-8}$ . This should be compared to the strain of a “typical” grain, i.e. a glass sphere with a 100 micron diameter, under just its own weight on the Earth’s surface:  $\delta/d \approx (\rho g d/E)^{2/3}$ . With the Young’s Modulus  $E \approx 6 \cdot 10^{10}$  Pa,  $\rho \approx 2 \cdot 10^3$  kg/m<sup>3</sup> and  $g \approx 10$  m/s<sup>2</sup>, this strain is about  $10^{-7}$ . Thus, even if isostaticity is ultimately restored, the relevance of the hard-sphere limit for real granular systems is still questionable.

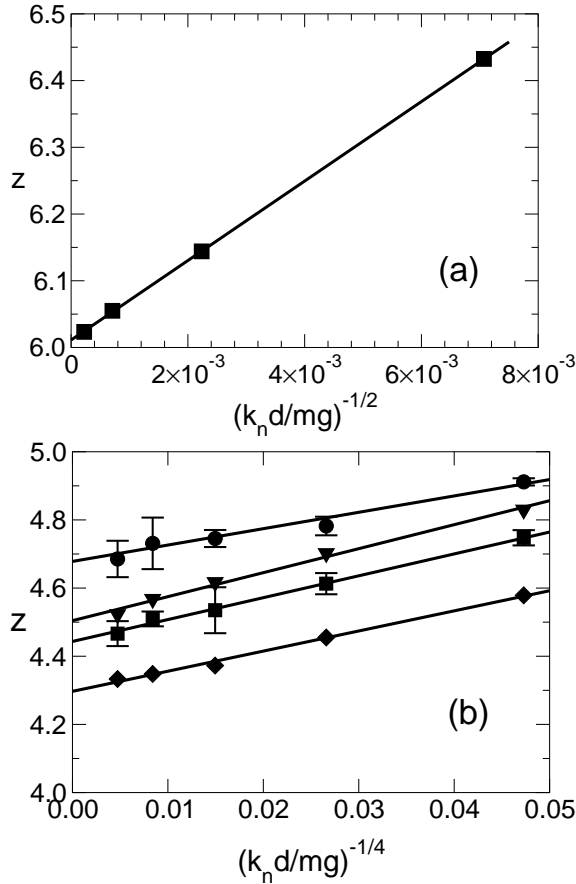


FIG. 7. Bulk averaged coordination number  $z$  as a function of particle hardness  $k_n$ , for  $\phi^i = 0.13$ : (a) For frictionless spheres, where the extrapolation to hard-spheres implies isostatic packing ( $z=6$ ); (b) For  $[\mu, \epsilon] = [0.50, 0.88]$  (solid circles),  $[0.50, 0.50]$  (triangles),  $[0.50, 0.26]$  (solid squares), and  $[10.0, 0.26]$  (solid diamonds), where the hard-sphere limit leaves the packings hyperstatic, with coordination numbers that depend on  $\mu$  and  $\epsilon$ .

#### D. Plasticity of Contacts

One potential explanation for the hyperstaticity of these frictional packings is the loss of degrees of freedom for the tangential forces in contacts that have become “plastic” such that  $F_t = \mu F_n$ . If a finite fraction of the contacts satisfied this condition, the isostaticity condition would need to be modified [8]. However, as demonstrated by the distribution of the plasticity index  $\zeta \equiv \frac{F_t}{\mu F_n}$  of the contacts in Fig. 8, almost all contacts in the static packings are below their frictional threshold  $\zeta = 1$ , eliminating this possibility. A similar distribution of  $\zeta$  was observed for a static packing created from flow arrest [8].

For  $\mu \geq 1$ , the distribution of the contact force ratio  $F_t/F_n$  indeed becomes independent of  $\mu$ , which manifests itself as a collapse of  $P(\zeta)$  when plotted against  $F_t/F_n$  (not shown). This result is in accord with the observa-

tion in Sec. III A that packings in this range of  $\mu$  behave effectively the same as for systems with  $\mu = \infty$ .

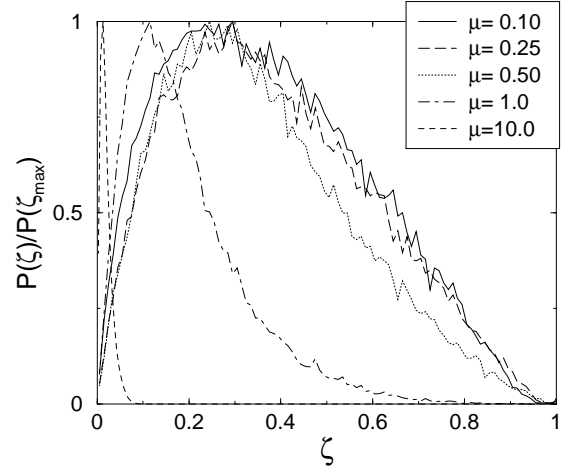


FIG. 8. Probability distribution  $P(\zeta)$ , normalized by its maximum value, for various values of  $\mu$ . Curves for  $\mu \geq 1$  would collapse if plotted against  $F_t/F_n$  instead of  $\zeta$ .

#### E. Effect of dissipation and initial conditions

The dependence of the packing geometry on coefficient of restitution  $\epsilon$  is also interesting. Unlike  $k_n$  and  $\mu$ , changing  $\epsilon$  would not change the configuration of a static packing after it has stopped – it only affects the relaxation dynamics by increasing the removal rate of kinetic energy. In this sense, changing  $\epsilon$  is like changing the quench rate of a supercooled liquid as it undergoes a glass transition. For very large quench rates, the system might be expected to stop immediately upon forming the minimum number of contacts necessary to achieve static mechanical equilibrium.

Similarly to the effect of  $\epsilon$ , we find that the initial starting densities also affect the final packing. In Fig. 9 we plot the variation in the final packing fraction  $\phi^f$ , and coordination number  $z$ , as a function of the starting density  $\phi^i$ . We find that more dilute starting states lead to more compact final states. This behaviour may be due to the increase in potential energy the system receives when it is more dilute, converting into kinetic energy of the particles during settling, and enabling them to explore more of the phase space on their way to achieving a preferred packing. An empirical fit to the packing fraction is given by,

$$\phi^f = 0.5778 + 0.0567 \exp(-4.3\phi^i), \quad (9)$$

which is similar to the empirical fit for model 2D systems proposed in Ref. [17]. However, it should be noted that for frictional spheres, extrapolation of the coordination number to the limit  $\phi^i = \phi^f$  does not result in isostaticity as observed in Ref. [17].

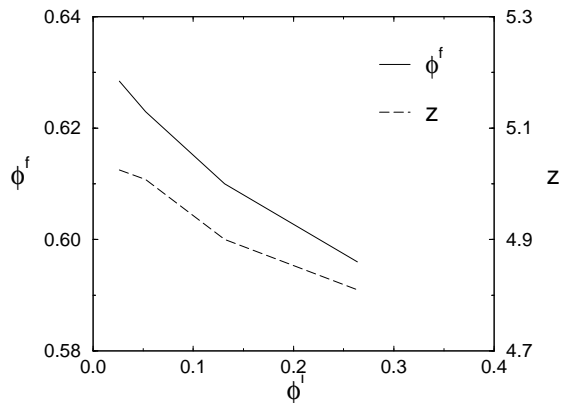


FIG. 9. Dependence of the final packing fraction  $\phi^f$  and coordination number  $z$  on the initial packing fraction of the falling particles  $\phi^i$ , for  $k_n = 2 \cdot 10^5 mg/d$ ,  $\epsilon = 0.88$ , and  $\mu = 0.50$ .

In light of the dependence of the final state on such parameters as  $\epsilon$  and  $\phi^i$ , the breakdown of the exponent identity Eq.(8) for frictional packings is perhaps not surprising. Packings obtained by the sedimentation of hard-spheres followed by elastic relaxation are probably not statistically equivalent to packings of particles that are elastic from the start, due to the strong history-dependence of the final states obtained.

In general, for hyperstatic packings the force network is not uniquely determined by the packing and the loadings on the particles. It follows that the determination of the force network for hyperstatic packings of perfectly rigid particles is an ill-posed problem [18]. Thus the order of the limit  $k_n \rightarrow \infty$  and the preparation of the packing cannot be commuted for frictional spheres. More bluntly, perfectly rigid sphere systems with friction are unlikely to capture the mechanical properties of packings of frictional, elastic spheres, even in the limit of extremely large rigidity of these latter particles.

#### IV. CONCLUSIONS

We have studied large scale packings of spherical grains of varying hardness, friction coefficient, and coefficient of restitution, formed by sedimentation. We accounted for the systematic variation with particle stiffness and were able to infer properties of hard-sphere packings. Although frictionless hard-spheres appear to form isostatic packings regardless of construction history and restitution coefficient, frictional packings achieve a multitude of hyperstatic packings that depend on system parameters and construction history [19]. The coordination number reduces smoothly from  $z = 6$  as the friction coefficient is increased, contrary to the hypothesis of isostaticity in such packings.

#### ACKNOWLEDGMENTS

Sandia is a multiprogram laboratory operated by Sandia Corporation, a Lockheed Martin Company, for the United States Department of Energy under Contract DE-AC04-94AL85000. DL acknowledges support from US-Israel Binational Science Foundation Grant 1999235.

- [1] C. A. Angell, K. L. Ngai, G. B. McKenna, P. F. McMillan, and S. W. Martin, J. App. Phys. **88**, 3113 (2000).
- [2] J. Liu, D. A. Weitz, and B. J. Ackerson, Phys. Rev. E **48**, 1106 (1993).
- [3] T. G. Mason, M.-D. Lacasse, G. S. Grest, D. Levine, J. Bibette, and D. A. Weitz, Phys. Rev. E **56**, 3150 (1997).
- [4] S. Alexander, Phys. Rep. **296**, 65 (1998).
- [5] S. F. Edwards, Physica A **249**, 226 (1998).
- [6] S. F. Edwards and D. V. Grinev, Physica A **263**, 545 (1999).
- [7] H. A. Makse, D. L. Johnson, and L. M. Schwartz, Phys. Rev. Lett. **84**, 4160 (2000).
- [8] L. E. Silbert, D. Ertas, G. S. Grest, T. C. Halsey, and D. Levine, cond-mat/0109124 (unpublished).
- [9] C. S. O'Hern, S. A. Langer, A. J. Liu, and S. R. Nagel, cond-mat/0110644.
- [10] We use Hookean springs as opposed to the more realistic Hertzian force law since for Hookean springs the coefficient of restitution  $\epsilon$  is constant, whereas it is velocity-dependent for Hertzian spheres. Consequently, it is far easier to drain residual kinetic energy from Hookean systems en route to a static packing. We have also studied some systems with Hertzian contacts. We found that our main conclusion that the coordination number reduces smoothly from six with increasing friction holds.
- [11] O. R. Walton and R. L. Braun, J. Rheo. **30**, 949 (1986).
- [12] P. A. Cundall and O. D. L. Strack, Géotechnique **29**, 47 (1979).
- [13] L. E. Silbert, D. Ertas, G. S. Grest, T. C. Halsey, D. Levine, and S. J. Plimpton, Phys. Rev. E **64**, 051302 (2001).
- [14] J. Schafer, S. Dippel, and D. E. Wolf, J. Phys. I France **6**, 5 (1996).
- [15] J. G. Berryman, Phys. Rev. A **27**, 1053 (1983).
- [16] S. Torquato, private communication. The abundance of such near-contacts is puzzling. A more detailed investigation of the origin of this singularity, using a common-contact analysis akin to the common neighbor analysis described in Ref. [20], but with a cutoff distance of  $r_c = 1^+$ , is beyond the scope of this study.
- [17] R. Blumenfeld, S. F. Edwards, and R. C. Ball, cond-mat/0105348.
- [18] T. C. Halsey and D. Ertas, Phys. Rev. Lett. **83**, 5007 (1999).
- [19] We also find similar results using Hertzian contacts.
- [20] A. S. Clarke and H. Jonsson, Phys. Rev. E **47**, 3975 (1993).